Impact of filler content on three-dimensional printed dental resins: A comparative study for provisional and permanent restorations

Seong-Keun Cho

The Graduate School
Yonsei University
Department of Industrial Dentistry

Impact of filler content on three-dimensional printed dental resins: A comparative study for provisional and permanent restorations

A Master's Thesis Submitted
to the Department of Industrial Dentistry
and the Graduate School of Yonsei University
in partial fulfillment of the
requirements for the degree of
Master of Science in Dentistry

Seong-Keun Cho

December 2024

This certifies that the Master's Thesis of Seong-Keun Cho is approved

Thesis Supervisor Jong-Eun Kim

Thesis Committee Member Jee-Hwan Kim

Thesis Committee Member Hyeon-Jong Lee

The Graduate School
Yonsei University
December 2024

감사의 글

본 논문을 완성하기까지 저를 이끌어 주신 김종은 교수님께 무한한 감사의 말씀을 올립니다. 많이 부족한 저에게 따뜻한 격려와 가르침을 주신 덕분에 연구 과정과 논문 작성을 마무리할 수 있었습니다. 또한, 더 좋은 논문이 될 수 있도록 세심하게 조언해주신 김지환 교수님과 이현종 교수님께도 깊이 감사드립니다.

바쁘신 중에도 함께 고민하고 노력해주시며 중요한 시점마다 아낌없는 조언을 해주신 임정화 선생님께 감사드립니다. 많은 것을 배울 수 있었고 연구 과정에서 큰 힘이 되었습니다. 이에 대한 감사의 마음을 이렇게나마 표현하고자 합니다.

소중한 연구의 결실을 맺을 수 있도록 배려해주시고 도와주신 회사의 동료분들께도 깊은 감사를 드립니다.

마지막으로, 변함없는 사랑으로 곁에서 묵묵히 지켜봐 주고, 항상 지지와 응원을 보내준 가족에게 진심으로 고마운 마음을 전합니다.

2024 년 12 월

조 성 근

TABLE OF CONTENTS

LIST OF FIGURES

LIST OF TABLES

ABSTRACT

Impact of filler content on three-dimensional printed dental resins: A comparative study for provisional and permanent restorations

Three-dimensional (3D) printing restoration materials used in the dental field are generally used as temporary restorations owing to their mechanical and physical limitations. Although various fillers affect the output, studies on the effect of filler content on 3D printing resin output are insufficient. Therefore, this study aimed to assess the effects of various filler content in 3D-printed resins on their mechanical and physical fitness in intermediate and final prosthetic designs. After designing a suitable specimen for the experiment, it was manufactured using five commercially available 3D printing resin materials and a CAD/CAM block for subtractive manufacturing (milling). The flexural strength, water absorption, solubility, and hardness were evaluated.

The flexural strength was markedly greater in resins with 50% or more filler content ($P<0.001$). However, the polymer-infiltrated ceramic network made by cutting did not show a significant difference from the low-filling resin group. The ceramic network of AMH imparted a nearly twofold higher surface hardness than that of the 3D-printed resin. Among the 3D-printed resins, the effect of the filler was significant, with Zir F showing the highest hardness followed by Cera F, whereas the other groups had similar hardness values.

These results show that a high filler content improves the mechanical properties, which provides insight into the reliability of materials; however, it is expected that detailed composition analysis and further research will be needed to fully explore the potential of high-charging 3D printing resins.

Key words : 3D-printed dental resins; filler content; mechanical properties; permanent restorations; provisional restorations

1. Introduction

Rapid and automated prototyping of dental materials and restorations in three dimensions (3D) technology has significantly affected the field of restorative dentistry in recent years. The advent of CAD/CAM technology, which seamlessly combines 3D imaging and manufacturing, has led to the adaptation of this modality in mainstream clinical dentistry (Tahayeri et al., 2018). Digitization using 3D methodologies has improved clinical efficiency (Jeong et al., 2023; Tian et al., 2021). In particular, the field of prosthodontics has benefited from the growth of high-accuracy 3D-printed restoration with advantages outweighing the more conventional milling options.

Extracoronal prosthetic restorative treatment typically involves a series of clinical and laboratory procedures. Restorations are termed interim or permanent based on the duration of application. Permanent restoration is the final restoration that lasts for an extended duration of several years, whereas interim restorations provide temporary functional and aesthetic support to the dental and interdental regions. Given the differences in their intended functions, the materials used for interim and permanent restorations also differ.

Although various materials have been proposed for interim restorations, the choice of permanent restorations remains relatively narrow. Metals, historically the material of choice, have been replaced in the past decade by ceramics and hybrid materials with excellent aesthetics and superior mechanical properties. However, the application of 3D-printed resin-based materials in permanent restorations remains uncommon. Biocompatible 3D printing resins that are commonly used clinically have properties that are inferior to those of conventionally used ceramic-based materials. Therefore, research interest in recent years has focused on enhancing the characteristics of 3D printing resins for suitability as permanent restorations.

Studies comparing 3D printing restorative materials with permanent milling materials have reported lower flexural strength and hardness with 3D printing resins. Therefore, various methods have been explored to improve the properties of 3D printing resins. One favorable approach is to

modify the filler phase of the composition. Material researchers have investigated the application of glass, silica, and zirconia by examining various parameters, including surface treatment, particle size, and dispersion techniques (Aati et al., 2021; AlGhamdi et al., 2024; Alshamrani et al., 2023). The incorporation of functionalized ZrO2 nanoparticles into 3D-printed acrylate ester-based resins significantly improved their mechanical properties, particularly the ductility, nanohardness, and flexural strength. The addition of 3 wt.% ZrO2 yielded optimal results, achieving the highest fracture toughness and elasticity (Aati et al., 2021). Resin parameters that can affect the viscosity and, in turn, printability have also been discussed. Low viscosity improves the flowability of the resin, enhances printability, and results in improved printing outcomes. An optimal filler viscosity promotes crosslinking within the polymer matrix, thereby enhancing the mechanical strength of the printed composites (Vyas et al., 2022). In summary, changes in the filler concentration, type, and proportion of the organic resin phase can enhance the properties of 3D-printed resins. However, its clinical applicability, particularly the suitability of such filler-augmented resins for permanent restorations, has not been tested or is scarcely reported.

A recent 2023 amendment to the definition of dental ceramic has removed the words “pressed, fired, polished, or milled” material (American Dental Association, 2023). Bypassing the manufacturing criteria from the definition of porcelain/ceramic allows 3D-printed ceramic crowns containing over 50% inorganic refractory compounds to be recognized as permanent restorations under CDT code D2740 (Bora et al., 2024). In other words, a proportional change in the filler content has improved the characteristics of the 3D-printed resin from interim to permanent restorations. However, these new materials are adequately benchmarked against materials commonly used in clinics. Furthermore, mapping the improvement in material properties against a comparable reference will contribute to evidence-based decision making in prosthetic dentistry. Polymer-infiltrated ceramic network (PICN) materials have shown promising clinical results with a variety of indications as an ideal criterion for associating novel 3D-printed composite resins with fatigue behavior and estimating clinical performance (Prause et al., 2024).

This study aimed to investigate the impact of different filler concentrations in the 3D printing resin on the mechanical and physical suitability of interim and final prosthesis designs. The present study compared the interim and recently introduced highly filled 3D printing dental resin with a hybrid CAD/CAM block as the reference. The null hypothesis stated that there would be no difference in the physical and mechanical properties of the 3D-printed dental resins based on the filler content.

2. Material and methods

2.1. Specimen fabrication

Five commercially available 3D printing resin materials for additive manufacturing (3D printing) and a CAD/CAM block for subtractive manufacturing (milling) as a reference group were used in this study (Figure 1). Information on the materials is summarized within the range provided by the manufacturer (Table 1).

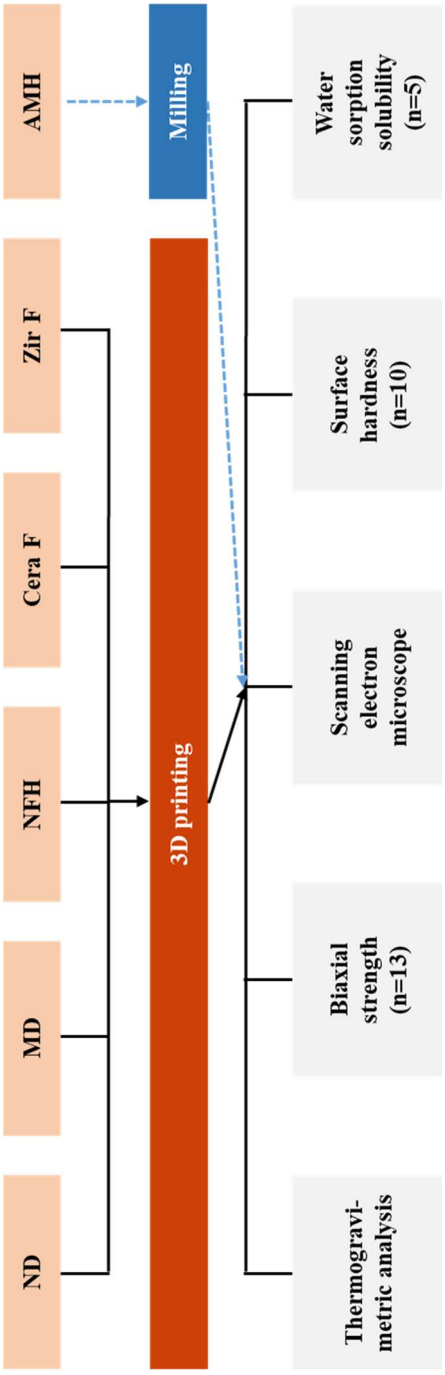

Figure 1. Study design and experiment flow

Table 1. Materials used in this study

	Material	**Group Code**	**Manufacturer**	**Filler characteristic[1]**	**Indicated Use**
Additive manufacturing (3D printing)	NextDent® C&B	ND	NestDent B.V. Netherlands	Unfilled	Crowns & Bridge
	Mazic D Temp	MD	VERICOM, South Korea	Unfilled	Crowns & Bridge
	C&B NFH Hybrid	NFH	ARUM DENTISTRY, South Korea	Low filled (<50%)	Fixed restoration
	RODIN™ Sculpture 1.0	Cera F	Pac-Dent, United State	Highly filled (>50%)	Fixed restorations and long-term provisional
	RODIN™ Sculpture 2.0	Zir F	Pac-Dent, United State	Highly filled (>60%)	Fixed restorations and long-term provisional
Subtractive manufacturing (Milling)	Amber® Mill H	AMH	HAAS, South Korea	Ceramic network	Fixed restorations

In this study, additive manufacturing was used to design the specimens using a freely available online CAD program (Thinkercad, Autodesk, San Rafael, California, USA) according to the specifications required for each test. The design file extracted in STL format was code-converted in a slicing program (Asiga Composer, Asiga, Sydney, Australia) by setting it to be stacked in a direction parallel to the floor with 50 μm per layer. The specimen was produced using a DLP type 3D printer with a 350 nm UV LED light source (Asiga MAX 385 UV, Asiga, Sydney, Australia). The liquid resin remaining around the printed specimen was washed in ethyl alcohol (95%) twice for 3 min each. The unpolymerized resin on the specimen's surface was further polymerized at 60 °C for 30 minutes in post-curing equipment using a 405 nm UV LED light source (Form Cure, Form labs, Massachusetts, United States).

On the other hand, for cutting processing, the designed file was uploaded to the CAM software (Apex Mill, ARUM Dentistry, South Korea) provided by the manufacturer to calculate the processing path, and the specimen was produced by cutting the block under water cooling using a 5-axis cutting machine (5X-500, ARUM Dentistry, South of Korea).

2.2. Biaxial flexural strength (BFS)

BFS testing was carried out in accordance with the guidelines of ISO 6872, utilizing a universal testing machine (Instron 3366, Instron, Norwood, MA, USA) with a crosshead speed set at 1 mm/min and employing a cylindrical steel piston with a diameter of 1.2 mm. The specimens were placed on a three-ball support system, where the balls had a diameter of 2.5 mm and the support diameter was 9 mm. The specimens were 14 mm in diameter and 2 mm in height, with 13 for each group. The biaxial flexural strength σ was calculated according to the following equation:

$$\sigma = -0.2387\ P\ (X - Y)/b^2$$

where σ is the maximum center tensile stress, in megapascals; P is the total load causing fracture, in newtons; and b is the thickness of the specimens at the origin of fracture. X and Y are as follows:

$$X = (1 + v)\ In\ (r_2 / r_3)^2 + [1 - v)/2]\ (r_2 / r_3)^2$$
$$Y = (1 + v)\ [1 + In(r_2 / r_3)^2] + (1 - v)\ (r_{1\,/}\, r_3)^2$$

where r_1 is the radius of the circle defined by the three balls, r_2 is the radius of the loaded area, r_3 is the radius of the specimen, and ν is the Poisson's ratio defined to ν = 0.25.

2.3. Weibull probability analysis

The Weibull modulus (m) and characteristic strength (σ, stress level at which 63.2% of specimens are expected to fail) were calculated for each material. The biaxial strength data were sorted in increasing order to assign ranks ranging from 1 to N (N is the number of specimens). A straight line was subsequently fitted to these points utilizing median-rank regression. The Weibull modulus was calculated as follows:

$$\mathrm{P}\ (\sigma) = 1 - \exp(-\sigma/\sigma_0)^m$$

where P(σ) is the fracture probability; σ is the fracture strength at a given P(σ); σ_o is the characteristic strength; and m is the Weibull modulus, which is the slope of the ln (ln 1/1-P) versus in σ plots.

2.4. Scanning electron microscope (SEM) and energy dispersive X-ray spectroscopy (EDS)

After performing the biaxial flexural strength test, the surface and cross-section of the fractured specimen were coated with gold using a Cressington 208HR Sputter Coater and then subjected to an SEM equipped with EDS (JEOL Ltd., JEOL-7800F, Tokyo, Japan) to observe the microstructure of the surface. To analyze the characteristics of the surface and cross-section of the specimen, it was observed at ×500, ×2,000, and ×10,000 magnification and an acceleration voltage of 10.0 kV.

To determine the chemical compositions of the fillers, an EDS system (AZtec, Oxford Instruments, Abingdon, Oxfordshire, UK) was used in different regions.

2.5. Thermogravimetric analysis (TGA)

TGA tests were performed in a simultaneous thermal analyzer (SDT 650, TA instrument, Delaware, USA) with a platinum pan (110 μL). The nitrogen flow was measured at a rate of 100 ml/min. The sample mass chosen for each experiment was 14–15 mg, so that the amount of resin was approximately the same in all experiments. The scans were performed at a rate of 10 °C/min in the temperature range of 10–900 °C.

2.6. Vickers hardness test

The manufactured specimens, 10 in each group, were wet polished sequentially with 1000, 2000, and 4000 grit (1000, SPDN-8P-1000; 2000, SPD-8P-2000; 4000, MSPDS-8P-4000; R&B,

South Korea). Each was measured three times with a microhardness measuring device (MMT-X, Matsuzawa, Akita, Japan), and the results were recorded as the Vickers hardness number (VHN). An indenter set at a 136° angle was pressed into the surface with a force of 300 gf for a duration of 15 seconds. The findings were presented as the mean value from all indentation points for each specimen.

2.7. Water sorption (Wsp) and solubility (Wsl)

In to assess water sorption and solubility (Wsp and Wsl), disk-shaped samples measuring 15 mm in diameter and 1 mm in thickness were analyzed in accordance with ISO 10477 (n=5). The placed in a glass desiccator filled with silica gel and kept at a temperature of 37 °C for 24 hours. They measured using an analytical balance that has a precision of 0.001 grams. This drying process was repeated until a consistent mass (m1) was achieved. The volume of each sample was then determined with a high-precision digital caliper. Subsequently, the dried samples were submerged in water and maintained at 37 °C, with their mass measured every 7 days until they reached a stable mass (m2). Finally, the samples were dried once more in a desiccator, and the procedure was repeated until a final stable mass (m3) was obtained. The values of wsp and wsl were calculated in micrograms per cubic millimeter using specified formulas:

:

$$w_{sp} = \frac{m_{2-m_3}}{V}$$

$$w_{sl} = \frac{m_{1-m_3}}{V}$$

2.8. Statistical analysis

All evaluations were conducted with SPSS software (version 27.0, SPSS Inc., Chicago, IL, USA). The Shapiro-Wilk test was utilized to evaluate the normality of the data, with a significance threshold established at 0.05.

For variables such as biaxial flexural strength, Vickers hardness, Wsp, and Wsl, one-way analysis of variance (ANOVA) was employed to determine if significant differences existed between the groups. Post hoc comparisons were conducted using Bonferroni correction. The relationship between Wsp and Wsl was further examined using Pearson's correlation analysis to identify significant associations between these variables. Statistical significance was set at a level of 0.05, and results with p-values below this threshold were considered statistically significant.

3. Results

3.1. Biaxial flexural strength

The biaxial flexural strength results indicate that Zir F (220.35 ± 12.31 MPa) demonstrated a statistically significantly ($P<0.001$) higher strength compared to the other groups (Figure 2). Cera F (203.50 ± 16.86 MPa) exhibited the second highest strength, which was statistically significant ($P < 0.001$) when compared to AMH (186.41 ± 9.47 MPa), NFH (182.74 ± 2.58 MPa), MD (179.35 ± 3.40 MPa), and MD (174.90 ± 6.06 MPa). While in the biaxial flexural strength were noted among ND, MD, NFH, and AMH, these variations did not reach statistical significance.

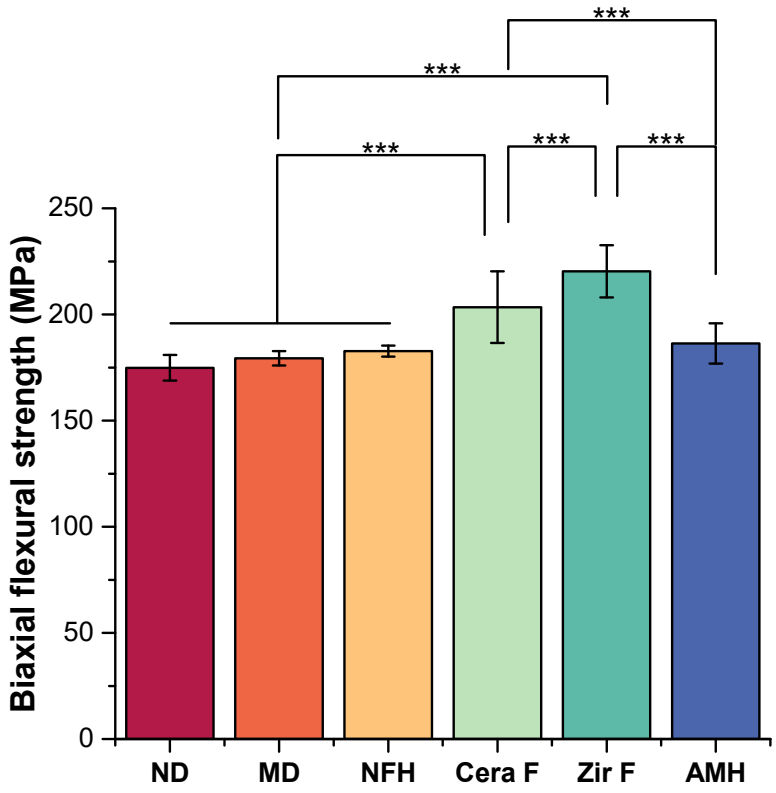

Figure 2. Biaxial flexural strength graph: one-way ANOVA result

3.2. Weibull probability analysis

The Weibull probability plots revealed a linear relationship between the natural logarithm of the failure probability and the natural logarithm of the applied stress across all material groups. The NFH and MD groups exhibited a rapid increase in the failure probability at higher stress levels, as indicated by the steepest slopes. In contrast, ZirF, Cera F, and AMH showed more gradual slopes, whereas ND showed moderate behavior with a steady increase (Figure 3).

The Weibull modulus (m), which indicates failure behavior, was the highest for NFH (69.96) and MD (60.93), followed by ND (36.10), AMH (23.95), ZirF (22.57), and Cera F (14.01). The scale parameters of the characteristic strengths of ZirF, Cera F, AMH, NFH, MD, and ND were 225.74, 211.07, 190.69, 184.01, 180.91, and 177.63, respectively, with lower values corresponding to earlier failures.

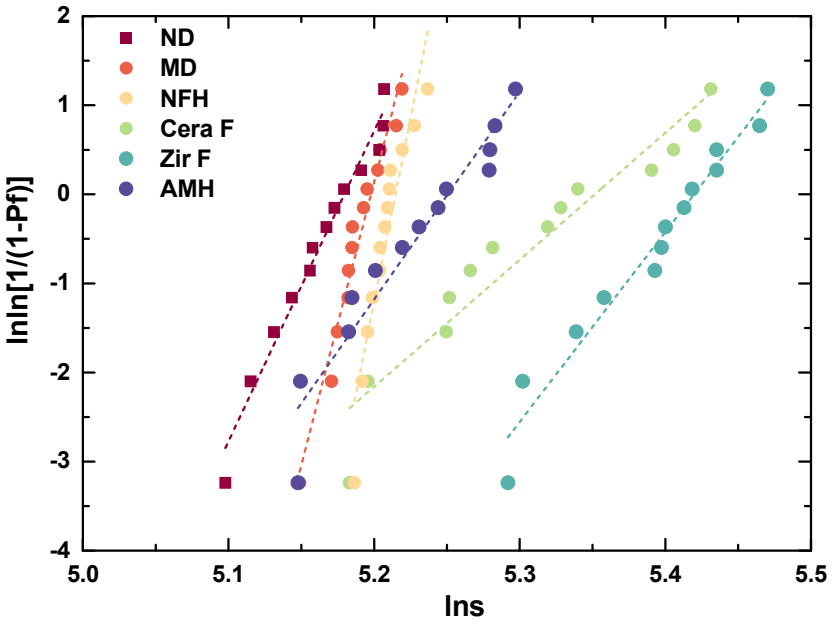

Figure 3. The Weibull probability plot for different materials is represented by the linearized relationship between the natural logarithm of the failure probability (lnln[1/(1 - Pf)]) and the natural logarithm of the applied stress (lnσ). The plot illustrates the Weibull distribution of the experimental groups, with data points fitted to a dashed line representing the trend based on their respective Weibull moduli. The spread and slope of the fitted lines provide insights into the mechanical reliability and strength variability of each material.

3.3. Surface morphology and fractography analysis

SEM microstructural analysis revealed characteristically different patterns among the various 3D-printed resin samples (Figure 4). Samples reinforced with higher filler contents, specifically Cera F, Zir F, and AMH, exhibited rougher surfaces and brittle fracture characteristics (cross-sections). By contrast, the ND, MD, and NFH samples, which had lower filler contents, had smoother surfaces and demonstrated a ductile fracture mode.

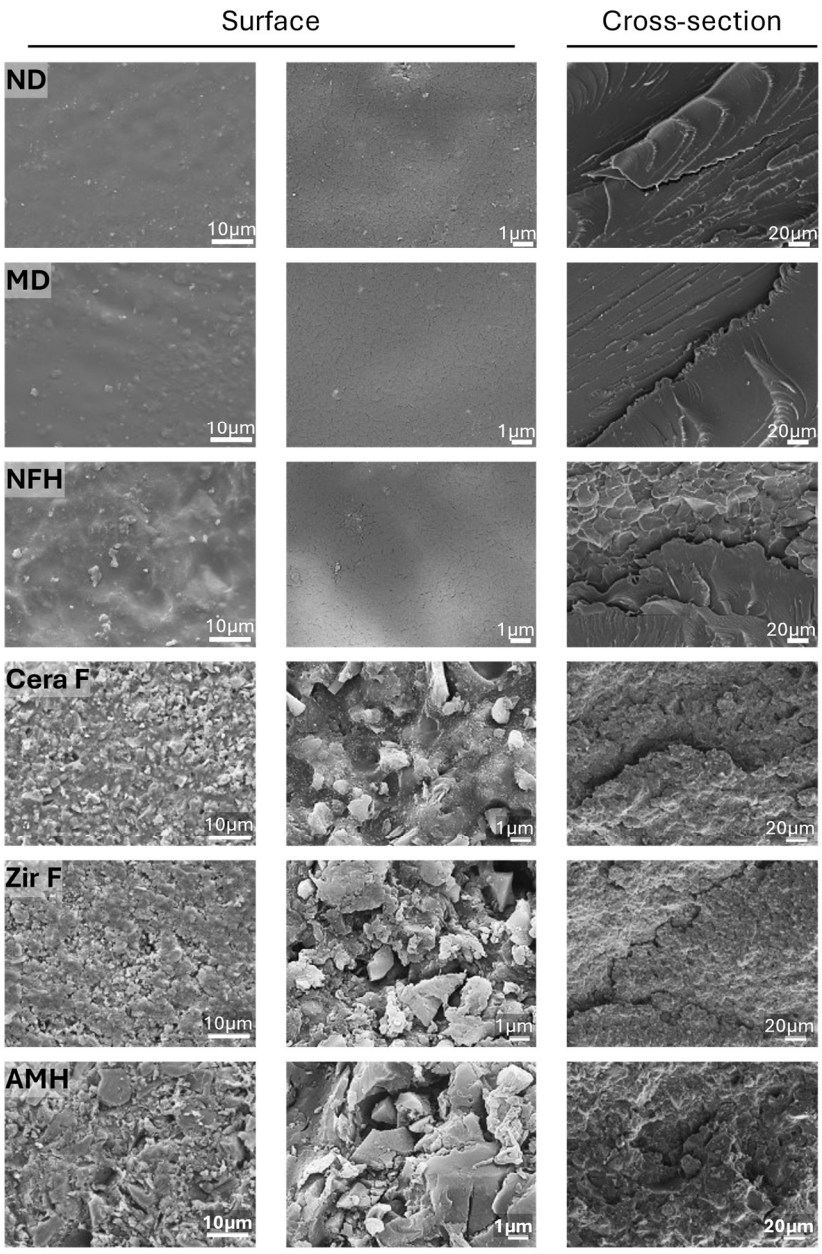

Figure 4. The surface is the region of the top of the 3D printing layers (left; magnification ×2,000, right; magnification ×10,000). Cross section of fractured surface after biaxial flexural strength (magnification ×500).

3.4. Thermal stability and filler spectroscopy

Figure 5A shows the TGA thermograms, indicating that Cera F, Zir F, and AMH exhibited high thermal stability, retaining 51–73 wt.% of their mass above 800 °C and maintaining over 50 wt% up to 900 °C, despite decomposition beginning around 300 °C. In contrast, ND, MD, and NFH displayed low thermal stability, retaining only 0–2 wt.% above 800 °C and undergoing nearly complete mass loss (<10%) starting at 450 °C. Specifically, NFH began decomposing at 248 °C, while ND and MD decomposed rapidly at 331 °C and 352 °C, respectively.

Spectroscopic characterization revealed the relative distribution of inorganic elements across all the experimental groups (Figure 5B, Table 2). Silicon (Si) was absent in the ND, MD, and NFH groups, but was detected in the Cera F, Zir F, and AMH groups. Both the Cera F and Zir F groups demonstrated an increased presence of barium (Ba), in addition to Si and aluminum (Al) (Figure 5C). The presence of zirconium (Zr) was confirmed in the Zir F group but was undetectable in the other groups. The AMH group exhibited the highest relative distribution of Si, followed by potassium (K), Al, and phosphorus (P).

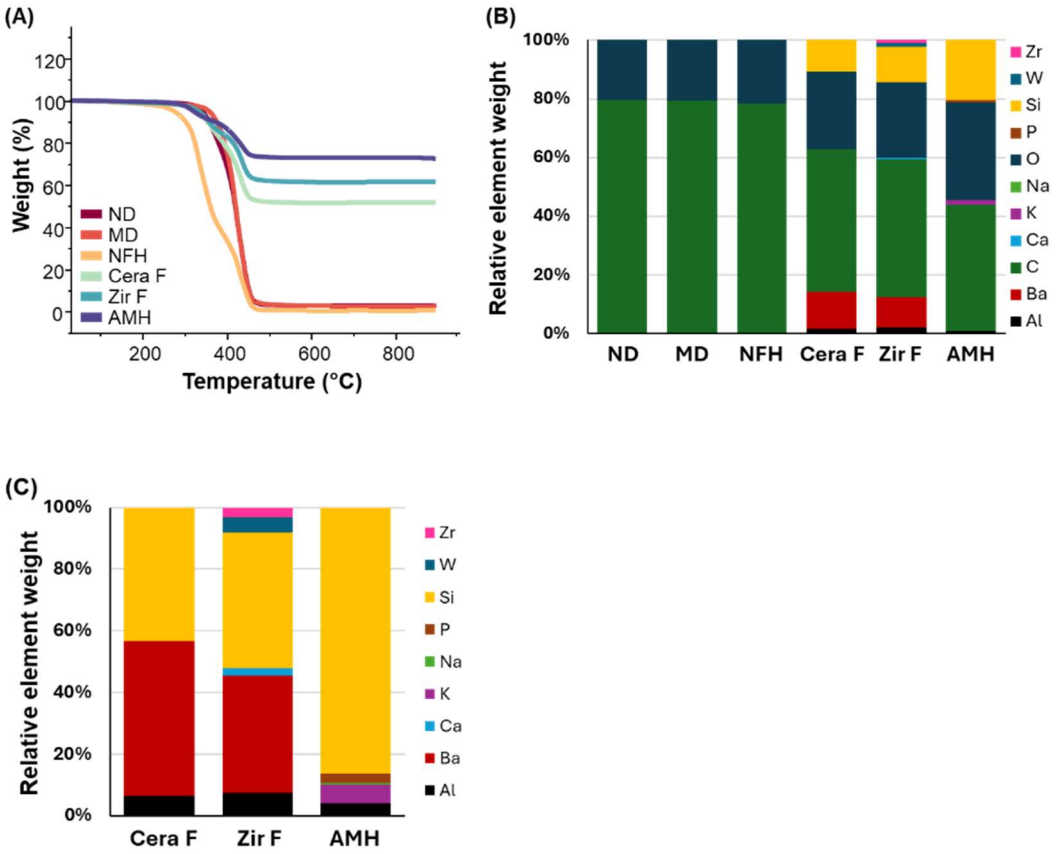

Figure 5. Characterization of filler content in the experimental groups. (A) Thermogravimetric analysis of the inorganic fraction in the polymerized samples. (B-C) Spectroscopic characterization showing the relative distribution percentages of different elements (B) across all experimental groups and (C) within the high filler loading groups.

Table 2. Elemental distribution from energy dispersive X-ray spectroscopy (EDS) analysis of experiment groups.

Group	Al	Ba	C	Ca	K	Na	O	P	Si	W	Zr
ND	0	0	79.74	0	0	0	20.27	0	0	0	0
MD	0	0	79.25	0	0	0	20.75	0	0	0	0
NFH	0	0	78.3	0	0	0	21.71	0	0	0	0
Cera F	1.63	12.53	48.78	0	0	0	26.31	0	10.76	0	0
Zir F	2.12	10.55	45.95	0.69	0	0	26.2	0	12.2	1.39	0.91
AMH	0.99	0	43.05	0	1.41	0.17	33.15	0.73	20.5	0	0

3.5. Surface hardness

The surface hardness evaluation showed slight variation but no statistical significance between the NFH (14.37 ± 2.63), ND (16.35 ± 0.57), and MD (16.46 ± 1.16) groups (Figure 6). However, the ND, MD, and NFH groups displayed significant differences compared to the Cera F (29.10 ± 2.26), Zir F (37.59 ± 3.05), and AMH (73.97 ± 7.23) groups. Among the latter, AMH exhibited the highest surface hardness, with significant differences ($P<0.001$) between Cera F, Zir F, and AMH.

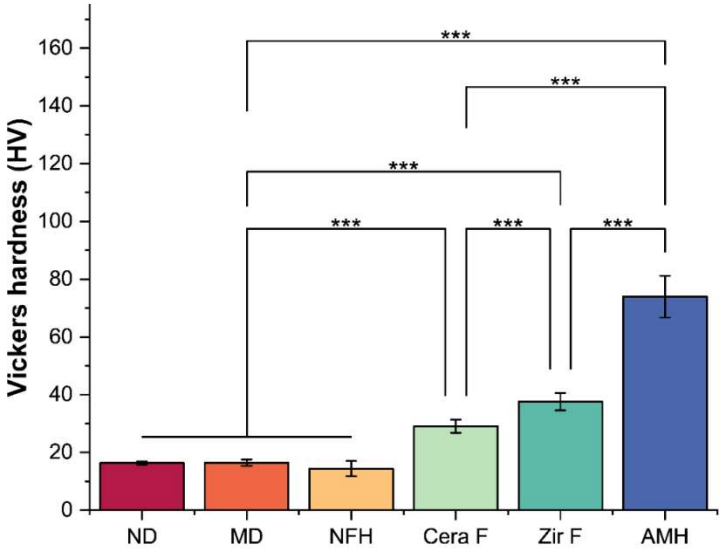

Figure 6. Post hoc test result graph in Bonferroni for Vickers hardness (*P < 0.05, ** P < 0.01, *** P < 0.001)

3.6. Water sorption and solubility

Table 3 presents the significant differences ($P < 0.001$) observed in the intergroup comparisons of Wsp and Wsl. NFH (29.20 ± 0.48 μg/mm³) and Zir F (29.66 ± 0.8 μg/mm³) exhibited the highest Wsp values, while ND (12.33 μg/mm³) and MD (11.85 μg/mm³) had the lowest. Additionally, NFH (3.82 ± 0.91 μg/mm³) demonstrated significantly higher Wsl values. In contrast, AMH (-1.53 ± 0.42 μg/mm³) showed the lowest Wsl among the groups. There no notable differences in Wsl observed among ND, MD, Cera F, and Zir F.. Furthermore, a notable positive correlation was observed between Wsp and Wsl, except for Zir F and AMH.

Table 3. Water sorption (Wsp) and solubility(Wsl)

Groups	W_{sp} (μg/mm^3)	W_{sl} (μg/mm^3)	Pearson correlation analysis (r)
ND	12.33 ± 0.41^{c}	-0.05 ± 0.37^{bc}	0.949**
MD	11.85 ± 0.39^{c}	0.99 ± 0.43^{b}	0.914*
NFH	29.20 ± 0.48^{a}	3.82 ± 0.91^{a}	0.979**
Cera F	18.33 ± 0.87^{b}	0.24 ± 1.11^{b}	0.950**
Zir F	29.66 ± 0.82^{a}	-0.05 ± 0.46^{bc}	0.280
AMH	17.57 ± 0.51^{b}	-1.53 ± 0.42^{c}	0.604
P-value	<0.0001	<0.0001	

Differences in lowercase letters within the same column indicate statistically significant differences.

Correlation analysis: * P<0.05, ** P<0.001

4. Discussion

The first 3D printing resins introduced for dental prosthesis fabrication demonstrated improved mechanical properties compared to conventional provisional restoration materials (Beyabanaki et al., 2023; Tahayeri et al., 2018). However, these enhancements were modest, limiting their use primarily to provisional fixed prostheses. Recently, new high-filled 3D printing resins offering significantly greater mechanical strength have been developed. To evaluate the scope of their application, the present study compared the new high-filled 3D printing dental resins with currently preferred clinical resins, using a hybrid PICN CAD/CAM block as a reference. The results revealed significant differences in the mechanical properties of the 3D-printed resins that were related to the proportion of filler content. Therefore, the hypothesis that a higher filler proportion in a 3D printing resin can enhance its physical and mechanical properties is supported.

The flexural mechanical behavior of fixed prosthetic materials is crucial for assessing the overall material strength (Saini et al., 2024; Valenti et al., 2024). In the present study, the biaxial flexural strength was evaluated, accounting for multidirectional loading and parafunctional movements within the oral cavity (Beyabanaki et al., 2023). The Cera F and Zir F high-filled resin groups exhibited higher strengths, with Zir F demonstrating the highest biaxial flexural strength. The increased strength of Zir F may be attributed to the nanoscale fillers incorporated within the material, which likely improve its tolerance to internal stress (Aati et al., 2021; Elfakhri et al., 2022). The strength of 3D-printed resins can be improved through factors such as adding fillers or nanofillers, printing orientation and angulation, printing layer thickness, and post-polymerization time and temperature (Gad and Fouda, 2023). Several have shown that the orientation of printing has a considerable impact on the flexural strength of resins produced through 3D printing. Generally, higher flexural strength is observed in the horizontal orientation than in the vertical orientation

(KEßLER et al., 2021; Unkovskiy et al., 2018). When are printed in a vertical orientation, the load direction aligns with the printing direction, which frequently leads to decreased strength due to weak adhesion between the layers. The adhesion strength between layers is influenced by several factors, including the type of composite resin used, the dimensions of the adhesion surface, and the rate of polymerization. These elements together impact the flexural strength of products printed vertically (Derban et al., 2021; Shim et al., 2020; Unkovskiy et al., 2018). Reducing the thickness of printed layers enhances the flexural strength of 3D-printed object. Specimens was printed with a layer thickness set to 50 μm exhibit greater flexural strength than those produced with a thickness of 100 μm. This increase in strength can be explained by the better polymerization of thinner layers, which benefit from better light penetration, as the light intensity is more effectively preserved when moving from the surface into the resin bulk, unlike in thicker layers (Perea-Lowery et al., 2021). In this study, the output was performed using the parameter values recommended by the 3D printer manufacturer, depending on the resin being used. The ND, MD, and NFH low-filled resin groups showed flexural strength comparable to that of the PICN AMH. This finding differs from those of a previous study that reported higher biaxial flexural strength in PICN restorative materials, such as AMH (Beyabanaki et al., 2023; Prause et al., 2024). This behavior could be the result of the presence of unevenly distributed defects that can influence load transmission prior to fracture, particularly in the ceramic network of AMH (Nohut and Lu, 2012). To account for this, Weibull statistics were calculated to provide more clinically relevant information regarding the structural reliability and variability of material strength (Rodrigues et al., 2008).

Generally, a higher Weibull modulus indicates a narrower distribution of failure stresses, suggesting better reliability of a material's performance under stress (McCabe and Carrick, 1986). The results of the present study revealed significant variations in both strength and material reliability among the groups. Previous studies reported a Weibull modulus for PICNs ranging from 4.8 to 16.7, with these variations attributed to internal stresses and the ceramic network within the PICN (Beyabanaki et al., 2023; Prause et al., 2024). Additionally, the Weibull modulus for ceramics

usually falls between 5 and 15. Therefore, the values observed for the AMH may stem from a combination of differences in the manufacturing process and material structure (McCabe and Carrick, 1986). In other words, while milled AMH may exhibit a higher characteristic strength in the Weibull statistics than ND, its strength is less consistent. Moreover, the Zir F and Cera F groups demonstrated superior mechanical performance compared to the AMH group. In summary, the application potential of the highly filled Zir F and Cera F materials surpasses the current scope of PICN.

To enhance our understanding of the variability in the Weibull moduli, a microstructural analysis was conducted using SEM. Typically, the filler content affects both the surface texture and internal fracture mechanics. An increase in filler concentration leads to more irregular and brittle structures (Aboushelib and Elsafi, 2016). In other words, the mechanical characteristics and failure modes of 3D-printed resins are closely associated with their filler content, highlighting its critical role in determining their overall performance.

In agreement with these findings, the microstructural analysis revealed typical characteristics of the tested resin materials. The Cera F and Zir F groups exhibited markedly rough surface topography and brittle fracture patterns, in contrast to the smooth and ductile fracture patterns observed in the ND, MD, and NFH groups. Subsequent EDS analysis further confirmed the differences in filler composition. Specifically, variations in the filler content, particularly of glass silica and zirconia, significantly influenced both the surface topography and fracture behavior. Taken together, the spectroscopy results, observed topography, and the patterns of fracture provide insight into the variations in mechanical properties previously mentioned.

Earlier has shown that the characteristics of fillers have varied impacts on the alteration of dental resins. Although changes in filler characteristics have led to improvements in the mechanical properties, these effects have been inconsistent and are frequently accompa

nied by reduced material efficiency (Aati et al., 2021; Almedarham et al., 2024). Additionally,

challenges such as the formation of voids or pores, along with limited curing depth and degree of polymerization over time, have been observed (Aati et al., 2021).

The surface microhardness is commonly used to evaluate the resistance of a material to wear and permanent indentations (Mangal et al., 2020a; Mangal et al., 2020b). Additionally, hardness serves as an indirect indicator of polymerization depth, which depends on the balance between organic and inorganic components and is an important factor for ensuring the long-term reliability of 3D-printed resin-based prostheses (Ferracane, 1985; Zattera et al., 2024). The ceramic network of AMH imparted a nearly twofold higher surface hardness than that of the 3d-printed resin. Among the 3d-printed resins, the effect of the filler was significant, with Zir F showing the highest hardness followed by Cera F, whereas the other groups had similar hardness values. Hardness was improved by increasing the filler content (Aati et al., 2021). In line with these research findings, the high-filler-content resin groups, Zir F and Cera F, exhibited superior mechanical properties.

In addition to mechanical surface abrasion, Wsp and Wsl are essential for assessing the resistance of a material to the surrounding oral fluid. Resin-based materials are prone to hydrolytic degradation and expansion, which further influence their clinical longevity. Earlier studies have reported a near doubling of Wsp in a resin matrix containing fillers, attributed to additional water entrapment at the interface between the filler and matrix (Ferracane, 1985). Although 3D printing resins differ fundamentally from direct restorative composite resins, recent studies have shown similar behavior between the two materials (AlGhamdi et al., 2024; Prause et al., 2024; Zattera et al., 2024). In the present study, the NFH group exhibited the highest Wsp and Wsl values, suggesting high susceptibility to wet oral conditions. Although Zir F demonstrated a similar Wsp, a negative solubility value was observed until the end of the experiment. According to the dual-mode theory of Wsp, this negative solubility indicates low solubility and the presence of a remnant bound water mass (Bai et al., 2024). In other words, a lower mass of the unreacted resin fraction or hydrolytic byproducts was released from the 3D-printed resin.

Although in vitro tests do not simulate the actual clinical conditions, the results of the present

study offer insights into the possible extent of Wsp and Wsl in the oral cavity. These findings indicated that the structure and properties of a material can undergo significant changes. Although more research is needed to confirm the clinical correlation with in vitro results, it is important to recognize that absorption and release are ongoing processes that can affect material properties over time (Bai et al., 2024). Therefore, when choosing a long-term prosthesis, high Wsp and Wsl values should be considered, particularly in situations involving adverse parafunctional habits.

The clinical implications of this study indicate that high-filled 3D printing resins, such as Cera F and Zir F, have strength properties that exceed those typically associated with PICN. These resins may be particularly advantageous in clinical scenarios in which the prostheses must endure significant occlusal loads and require minimal flexural deformation, such as in the case of onlays, inlays, and fixed crowns. However, the lack of comprehensive compositional data from manufacturers limits the ability to directly correlate the filler content with the mechanical properties. Although Weibull statistics provide valuable insights into the reliability of these materials, the estimates may differ under cyclic loading conditions, such as those simulated by chewing. In addition, this study evaluated novel 3D-printed resins alongside PICN. A comparison of these materials with existing zirconia- and ceramic-based alternatives would provide valuable insights into their specific clinical applications. Future research should focus on detailed compositional analyses and broader comparative studies to fully explore the potential of high-filled 3D printing resins in dental prosthetics.

5. Conclusion

Within the limitations of this study, the following conclusions can be drawn:

1. The flexural characteristics and VHN of the 3D-printed resins improved with increasing filler content, indicating a close relationship between these parameters.
2. High-filler-content 3D-printed resins, specifically Cera F and Zir F, exhibited superior mechanical performance compared to AMH, a hybrid CAD/CAM block.
3. These findings support the hypothesis that increasing the filler content enhances the mechanical properties of 3D-printed resins. The significant differences observed in the strength and fracture behavior among the various groups further substantiate this claim.

References

Aati S, Akram Z, Ngo H, Fawzy AS (2021). Development of 3D printed resin reinforced with modified ZrO_2 nanoparticles for long-term provisional dental restorations. *Dental Materials* 37(6): e360-e374

Aboushelib MN, Elsafi MH (2016). Survival of resin infiltrated ceramics under influence of fatigue. *Dental Materials* 32(4): 529-534

AlGhamdi MA, Alatiyyah FM, Dawood ZHA, Alshaikhnasser FY, Almedarham RF, Alboryh SY, et al. (2024). Flexural strength of 3D-printed nanocomposite provisional resins: Impact of SiO_2 and ZrO_2 nanoparticles and printing orientations in vitro. *Journal of Prosthodontics.* Epub ahead of print

Almedarham RF, Al Dawood ZH, Alatiyyah FM, Akhtar S, Khan SQ, Shetty AC, et al. (2024). Flexural properties of additive manufactured resin designated for interim fixed dental prosthesis: Effect of nanoparticles, build direction, and artificial aging. *The Saudi Dental Journal*

Alshamrani A, Alhotan A, Kelly E, Ellakwa A (2023). Mechanical and biocompatibility properties of 3D-printed dental resin reinforced with glass silica and zirconia nanoparticles: In vitro study. *Polymers* 15(11): 2523

American Dental Association: Glossary of Dental Clinical Terms. (2023). United States: American Dental Association

Bai X, Chen Y, Zhou T, Pow EHN, Tsoi JKH (2024). The chemical and optical stability evaluation of injectable restorative materials under wet challenge. *Journal of Dentistry* 146: 105031.

Beyabanaki E, Ashtiani RE, Moradi M, Namdari M, Mostafavi D, Zandinejad A (2023). Biaxial flexural strength and Weibull characteristics of a resin ceramic material after thermal-cycling. *Journal of Prosthodontics* 32(8): 721-727.

Bora PV, Sayed Ahmed A, Alford A, Pitttman K, Thomas V, Lawson NC (2024). Characterization of materials used for 3D printing dental crowns and hybrid prostheses. *Journal of Esthetic and Restorative Dentistry* 36(1): 220-230.

Derban P, Negrea R, Rominu M, Marsavina L (2021). Influence of the printing angle and load

direction on flexure strength in 3D printed materials for provisional dental restorations. *Materials* 14(12): 3376

Elfakhri F, Alkahtani R, Li C, Khaliq J (2022). Influence of filler characteristics on the performance of dental composites: A comprehensive review. *Ceramics International* 48(19): 27280-27294

Ferracane JL (1985). Correlation between hardness and degree of conversion during the setting reaction of unfilled dental restorative resins. *Dental Materials* 1(1): 11-14.

Gad MM, Fouda SM (2023). Factors affecting flexural strength of 3D-printed resins: A systematic review. *Journal of Prosthodontics* 32(S1): 96-110

Jeong M, Radomski K, Lopez D, Liu JT, Lee JD, Lee SJ (2023). Materials and Applications of 3D Printing Technology in Dentistry: An Overview. *Dentistry Journal (Basel)* 12(1).

KEßLER A, Hickel R, Ilie N (2021). In vitro investigation of the influence of printing direction on the flexural strength, flexural modulus and fractographic analysis of 3D-printed temporary materials. *Dental materials journal* 40(3): 641-649

Mangal U, Min YJ, Seo JY, Kim DE, Cha JY, Lee KJ, et al. (2020a). Changes in tribological and antibacterial properties of poly(methyl methacrylate)-based 3D-printed intra-oral appliances by incorporating nanodiamonds. *Journal of the Mechanical Behavior of Biomedical Materials* 110: 103992.

Mangal U, Seo JY, Yu J, Kwon JS, Choi SH (2020b). Incorporating Aminated Nanodiamonds to Improve the Mechanical Properties of 3D-Printed Resin-Based Biomedical Appliances. *Nanomaterials (Basel)* 10(5): 827-827.

McCabe JF, Carrick TE (1986). A statistical approach to the mechanical testing of dental materials. *Dental Materials* 2(4): 139-142.

Nohut S, Lu C (2012). Fracture statistics of dental ceramics: Discrimination of strength distributions. *Ceramics International* 38(6): 4979-4990.

Perea-Lowery L, Gibreel M, Vallittu PK, Lassila L (2021). Evaluation of the mechanical properties and degree of conversion of 3D printed splint material. *Journal of the mechanical behavior of biomedical materials* 115: 104254

Prause E, Malgaj T, Kocjan A, Beuer F, Hey J, Jevnikar P, et al. (2024). Mechanical properties of 3D-printed and milled composite resins for definitive restorations: An in vitro comparison

of initial strength and fatigue behavior. *Journal of Esthetic and Restorative Dentistry* 36(2): 391-401.

Rodrigues SA, Jr., Ferracane JL, Della Bona A (2008). Flexural strength and Weibull analysis of a microhybrid and a nanofill composite evaluated by 3- and 4-point bending tests. *Dental Materials* 24(3): 426-431.

Saini RS, Gurumurthy V, Quadri SA, Bavabeedu SS, Abdelaziz KM, Okshah A, et al. (2024). The flexural strength of 3D-printed provisional restorations fabricated with different resins: a systematic review and meta-analysis. *BMC Oral Health* 24(1): 66.

Shim JS, Kim J-E, Jeong SH, Choi YJ, Ryu JJ (2020). Printing accuracy, mechanical properties, surface characteristics, and microbial adhesion of 3D-printed resins with various printing orientations. *The Journal of prosthetic dentistry* 124(4): 468-475

Tahayeri A, Morgan M, Fugolin AP, Bompolaki D, Athirasala A, Pfeifer CS, et al. (2018). 3D printed versus conventionally cured provisional crown and bridge dental materials. *Dental Materials* 34(2): 192-200.

Tian Y, Chen C, Xu X, Wang J, Hou X, Li K, et al. (2021). A Review of 3D Printing in Dentistry: Technologies, Affecting Factors, and Applications. *Scanning* 2021: 9950131.

Unkovskiy A, Bui PH-B, Schille C, Geis-Gerstorfer J, Huettig F, Spintzyk S (2018). Objects build orientation, positioning, and curing influence dimensional accuracy and flexural properties of stereolithographically printed resin. *Dental Materials* 34(12): e324-e333

Valenti C, Isabella Federici M, Masciotti F, Marinucci L, Xhimitiku I, Cianetti S, et al. (2024). Mechanical properties of 3D printed prosthetic materials compared with milled and conventional processing: A systematic review and meta-analysis of in vitro studies. *The Journal of prosthetic dentistry* 132(2): 381-391.

Vyas A, Garg V, Ghosh SB, Bandyopadhyay-Ghosh S (2022). Photopolymerizable resin-based 3D printed biomedical composites: Factors affecting resin viscosity. *Materials Today: Proceedings* 62: 1435-1439

Zattera ACA, Morganti FA, de Souza Balbinot G, Della Bona A, Collares FM (2024). The influence of filler load in 3D printing resin-based composites. *Dental Materials* 40(7): 1041-1046.

ABSTRACT IN KOREAN

충전제 함량이 3D 프린팅 치과용 수지에 미치는 영향: 임시 및 영구 보철물을 위한 비교 연구

치과분야에서 사용되는 3D 프린팅 수복 재료는 기계적 및 물리적 한계성으로 일반적으로 임시 수복물로 사용되고 있다. 다양한 필러가 출력 결과물에 영향을 미치고 있지만, 충전제 함량에 따른 3D 프린팅 레진 출력물에 어떠한 영향을 미치는지에 관한 연구는 부족하다. 따라서 본 연구는 3D 프린팅 레진의 다양한 필러 농도가 중간 및 최종 보철물 설계에서 기계적 및 물리적 적합성에 미치는 영향을 평가하고자 하였다. 실험에 적합한 시편을 디자인 한 후 적층 제조를 위한 상업적으로 이용 가능한 5 개의 3D 프린팅 수지 재료와 절삭(밀링) 재료를 사용하여 시편을 제작하였으며 굴곡강도, 수분 흡수도 및 용해도, 경도를 평가하였다. 그 결과 굴곡 강도는 충전제가 50% 이상 포함된 레진의 출력물에서 유의하게 더 높은 강도를 보였다. ($P<0.001$) 그러나 절삭를 통해 만든 PICN 내의 세라믹 네트워크 기반의 재료는 저충전 수지그룹과 유의한 차이를 나타내지 않았다. AMH 의 세라믹 네트워크는 3D 프린팅 레진에 비해 거의 2 배 더 높은 표면 경도를 보였다. 3D 프린팅 레진 중 필러의 효과는 Zir F 가 가장 높고 Cera F 가 뒤를 이어 다른 그룹이 유사한 경도 값을 갖는 것으로 유의하게 입증되었다. 본 연구의 한정된 결과에 따라 높은 충전제 함량이 기계적 특성을 개선하는 것으로 보이며, 이를 통해 재료의 신뢰성에 대한 통찰력을 제공하나 고충전 3D 프린팅 레진의 잠재력을 완전히 탐구하기 위해 상세한 조성 분석과 많은 연구가 필요할 것으로 기대된다.

핵심되는 말 : 3D 프린팅 치과용 수지, 충전제 함량, 기계적 특성, 영구 보철물, 임시 보철물